

# Analysis of Uniform-Strength Shape by the Growth-Strain Method\*

## (Application to the Problems of Steady-State Vibration)

Hideyuki AZEGAMI\*\*, Tadashi OGIHARA\*\*\*  
and Akiyasu TAKAMI\*\*

The growth-strain method, developed using the finite-element calculation of the deforming of shapes produced by swelling and contracting of itself, was previously proposed as a shape optimization method. The present report describes an application of the growth-strain method to the problems of steady-state vibration. In particular, free vibration with a normal mode and vibrational response to a harmonic excitation are considered. A difference of the implementation of the method for these vibration problems from that for static problems lies in analyzing the stress distribution at the deformation in the normal mode or in the amplitude of the vibrational response. Numerical examinations are carried out on simple beam structures. In these examinations, the growth-strain method shows a feasibility even in the optimization of structures under dynamic circumstances.

**Key Words:** Optimum Design, Computer-Aided Design, Eigenvalue Problem, Mode of Vibration, Finite-Element Method

### 1. Introduction

In the previous report<sup>(1)</sup>, one of the authors proposed a general-purpose method to analyze uniform strength shapes using the finite-element method, and obtained successful results to static elastic problems. In this report, we call the method the growth-strain method.

The focus in the following article will be on the application of the growth-strain method to the problems of steady-state vibration. In particular, free vibration with a normal mode and a vibrational response to harmonic excitation are considered. Our attention is on the analysis of uniform strength shape which is, to be exact, different from the analysis<sup>(2)-(9)</sup> of optimum shape with maximum natural frequency or minimum mass. The relation to these previous

works will be discussed in another report.

### 2. Growth-Strain Method

The growth-strain method is concisely formulated as follows<sup>(1)</sup>.

#### 2.1 Generation law of bulk strain

Let us consider the shape deformation of a solid body by swelling and contracting of itself. The deformation can be performed by generation of bulk strain positively and/or negatively in all parts of a body, and so we consider the generation law of the bulk strain.

Let us assume that the generation law of the bulk strain is given as a function of a growth parameter and consider what is appropriate to the growth parameter. To uniformize the strength of a solid body, it is proper to consider the uniform distribution of the strength parameter which is given, for example, by the Mises stress in the case of the Mises criterion or the maximum principal stress in the case of the maximum principal stress criterion. The strength parameter generally has the property of decreasing with increasing volume. Consequently, we assume that the strength parameter is employed for the growth parameter and that the bulk strain tensor  $\epsilon_{ij}^b$  is gener-

\* Received 19th December, 1990. Paper No. 89-1128A

\*\* Department of Energy Engineering, Toyohashi University of Technology, 1-1, Hibarigaoka, Tempaku-cho, Toyohashi 441, Japan

\*\*\* Suzuki Motor Company, Ltd., 330, Takatsuka, Kami-mura, Hamana-gun, Shizuoka-ken 432-91, Japan

ated in proportion with the deflection of the growth parameter  $p$  to its basic value  $p_0$  :

$$\epsilon_{ij}^B = \frac{p - p_0}{p_0} h \delta_{ij} \quad (1)$$

The tensor  $\delta_{ij}$  is the Kronecker delta. The constant  $h$  is called the growth rate with which the magnitude of bulk strain at a growth deformation process is determined. The basic value  $p_0$  is a design constant given as an objective value of  $p$ . Substituting the volume average of  $p$  into  $p_0$ , it is expected that the mass change is repressed, because the integral of  $\epsilon_{ij}^B \delta_{ij}$  in the volume becomes zero. On the other hand, substituting the maximum value of  $p$  into  $p_0$ , it is expected that the mass monotonously decreases, because  $\epsilon_{ij}^B$  is always negative.

**2.2 Growth deformation analysis**

The deformation to be generated by the bulk strain can be determined using the condition of the minimum strain energy. To distinguish the stress and strain at the deformation from those generated by acting external forces, we call the stress and strain the growth stress and the growth strain.

The strain energy  $U^G(u_i^G)$  caused by the bulk strain  $\epsilon_{ij}^B$  in a solid body with volume  $V^0$  at the natural state is given as a function of growth displacement  $u_i^G$  :

$$U^G(u_i^G) = \frac{1}{2} \int_{V^0} (\epsilon_{ij}^G - \epsilon_{ij}^B) D_{ijkl} (\epsilon_{kl}^G - \epsilon_{kl}^B) dV^0 \quad (2)$$

where the growth strain  $\epsilon_{ij}^G$  satisfies the equation of compatibility :

$$\epsilon_{ij}^G = \frac{1}{2} (u_{i,j}^G + u_{j,i}^G) \quad (3)$$

and  $D_{ijkl}$  is the stiffness tensor. The summation convention and the notation  $(\ )_{,i} = \partial(\ ) / \partial x_i^0$  are employed in the tensor expression, where  $x_i^0$  is the coordinate at the natural state.

The growth displacement  $u_i^G$  is determined from the minimum condition of  $U^G(u_i^G)$  :

$$\delta U^G(u_i^G) = \int_{V^0} (\epsilon_{ij}^G - \epsilon_{ij}^B) D_{ijkl} \delta \epsilon_{kl}^G dV^0 = 0 \quad (4)$$

where  $\delta$  denotes the virtual variation satisfying a boundary condition for the shape restriction. Using matrix expression, Eq. (4) becomes

$$\int_{V^0} \delta \{\epsilon^G\}^T [D] \{\epsilon^G\} dV^0 = \int_{V^0} \delta \{\epsilon^G\}^T [D] \{\epsilon^B\} dV^0 \quad (5)$$

The notation  $(\ )^T$  is the transposed.

Now, using the finite-element method, the growth strain vector  $\{\epsilon^G(x_i^0)\}_e$  at  $x_i^0$  in each element is expressed with the nodal growth displacement vector  $\{u^G\}_e$  :

$$\{\epsilon^G(x_i^0)\}_e = [B(x_i^0)]_e \{u^G\}_e \quad (6)$$

where  $[B(x_i^0)]_e$  is the stress-nodal displacement matrix. Expanding these element matrix  $[B(x_i^0)]_e$  and vectors  $\{\epsilon^G(x_i^0)\}_e, \{u^G\}_e$  into the entire matrix  $[B(x_i^0)]$

and vectors  $\{\epsilon^G(x_i^0)\}, \{u^G\}$  with every nodal component, superposing these expanded expressions for Eq. (6) and substituting them into Eq. (5), we obtain

$$\begin{aligned} \delta \{u^G\}^T \int_{V^0} [B(x_i^0)]^T [D] [B(x_i^0)] dV^0 \{u^G\} \\ = \delta \{u^G\}^T \int_{V^0} [B(x_i^0)]^T [D] \{\epsilon^B(x_i^0)\} dV^0 \end{aligned} \quad (7)$$

Consequently, the governing equation of the growth deformation is obtained by

$$[K] \{u^G\} = \{g\} \quad (8)$$

where the stiffness matrix  $[K]$  and the equivalent nodal force vector  $\{g\}$  generated by the bulk strain are given by

$$[K] = \int_{V^0} [B(x_i^0)]^T [D] [B(x_i^0)] dV^0 \quad (9)$$

$$\{g\} = \int_{V^0} [B(x_i^0)]^T [D] \{\epsilon^B(x_i^0)\} dV^0 \quad (10)$$

**2.3 Procedure**

The scheme of the growth-strain method is, as shown in Fig. 1, to iterate the two analytical steps of the stress analysis and the growth analysis using the finite-element method. The beginning and termination are with the stress analysis. Deformation and stress distribution under a mechanical boundary condition are evaluated in the stress analysis. The growth deformation is analyzed in the growth analysis under a boundary condition of shape restriction coming from the design strategy.

The convergence of the shape can be confirmed by comparing stress distributions before and after the growth analysis. The mesh refinement should be done after the growth deformation, if necessary.

**3. Application to Problems of Steady-State Vibration**

Typical problems of the steady-state vibration are given by a free vibration specified with each natural mode and a response to harmonic excitation. The characteristic common to them is the existence of the condition for the maximum deformation which is unique and independent of time. With change of the shape, this deformation continuously changes while maintaining its uniqueness and the independence of time. Consequently, it is considered to be optimal that

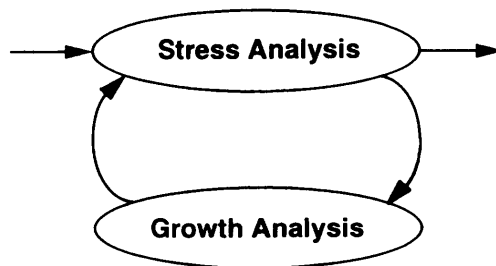


Fig. 1 Growth-strain method

the strength of the solid body would be uniformized by the growth analysis of the distribution of the strength parameter at the maximum deformation.

The three basic problems are provided as shown in Fig. 2. Cases 1 and 2 are for free vibration with a normal mode. In Case 1, a cantilever beam with nonstructural mass at the top is assumed. A free beam with nonstructural mass at both ends is assumed in Case 2. The response problem to harmonic excitation is treated in Case 3, where the same cantilever beam as in Case 1 is excited by harmonic shear loading at the top at a frequency lying between the 1st and 2nd natural frequencies. In all cases, the plane-stress condition is assumed, and the nonstructural mass and shear loading are assumed to be applied uniformly on these end-surfaces and do not change their total values.

The growth parameter  $p$  employed was the Mises stress  $\sigma$ . The volume average of  $\sigma$  was substituted into  $p_0$ . A value of 0.05 was assigned to the growth rate  $h$ . The eight-noded isoparametric elements were used. A mesh refinement to rearrange the inner nodes at a regular interval along the direction of width was performed in every case. In Case 3, before the rearrangement of the inner nodes, the nodes on the

surface was rearranged at a regular interval along the surface.

To check the computational details, we show the basic equations used in the analyses here. The mass matrix  $[M]$  and the stiffness matrix  $[K]$  with size  $N \times N$  are obtained by the standard procedure of the finite-element method. Neglecting damping, their matrices are related with the natural angular frequency  $\Omega_r$  and the normal mode  $\{\Phi_r\}$  of the  $r$ -th mode vibration:

$$(-\Omega_r^2[M] + [K])\{\Phi_r\} = [0] \quad (11)$$

$$\{\Phi_i\}^T [M] \{\Phi_j\} = \delta_{ij} \quad (12)$$

The amplitude vector  $\{U\}$  of displacement response to a harmonic excitation force with the amplitude vector  $\{F\}$  and frequency  $\omega$  is approximately given in terms of  $\Omega_r$  and  $\{\Phi_r\}$  summing up from the 1st to the  $m$ -th mode ( $m \ll N$ ), including rigid-body modes, if existent:

$$\{U\} = \sum_{r=1}^m \frac{[R]}{\Omega_r^2 - \omega^2} \{F\} \quad (13)$$

$$[R] = \{\Phi_r\} \{\Phi_r\}^T \quad (14)$$

where  $[R]$  is called the residue matrix. In Cases 1 and 2, the distribution of the strength parameter was evaluated at the deformation in the normal mode  $\{\Phi_r\}$ . The response to the harmonic excitation in Case 3 was

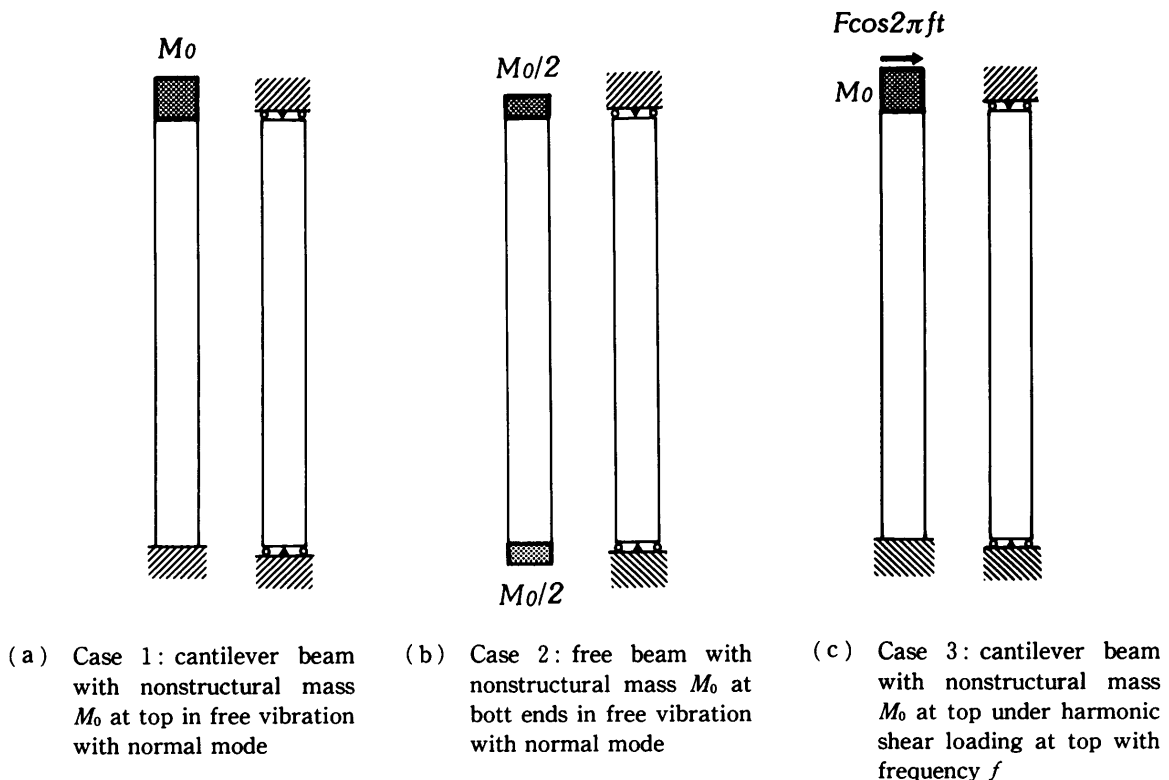


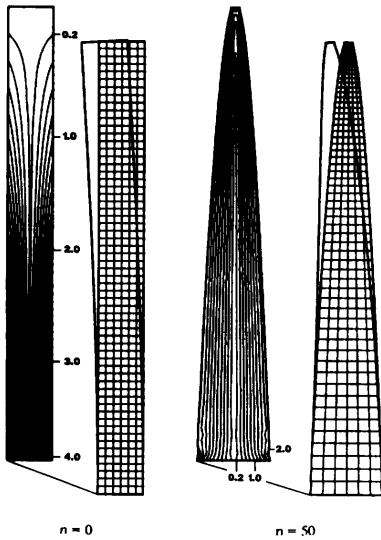
Fig. 2 Problems; left and right figures show boundary conditions for stress analysis and growth analysis, respectively; width = 6 m, length = 60 m,  $M_0$  = initial beam mass,  $F = 6$  MN/m,  $f = 500$  Hz; Young's modulus  $E = 210$  GPa, Poisson's ratio  $\nu = 0.3$ , density  $\rho = 7.8 \times 10^3$  kg/m<sup>3</sup>

given by Eq. (13), in which  $m=5$  was assumed and the 4th-mode of longitudinal mode was included.

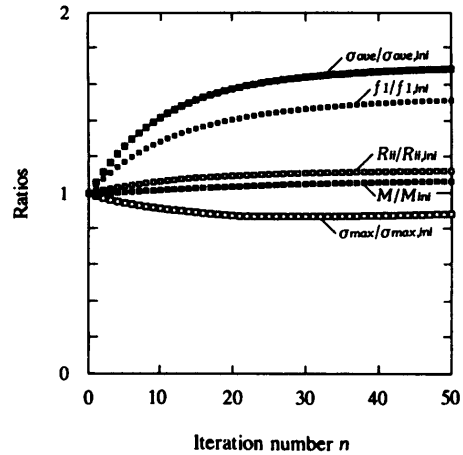
The results are shown in Figs. 3 and 4 for Case 1, and in Figs. 5 and 6 for Case 2. Figures 3 and 5 are for the 1st mode, and Figs. 4 and 6 are for the 2nd mode. In each case, the change of mass was repressed by using the volume average of strength parameter for  $p_0$  in Eq. (1). From the results of the maximum value of strength parameter obtained from iteration of the growth analysis, it is indicated that the strength

monotonously increased and converged to a certain value. In these problems, the natural frequencies increased monotonously and converged with respect to iteration of the growth analysis.

The results in the Case 3 of harmonic excitation are shown in Fig. 7. In this case, the each natural frequency changes with variation of shape, so that the contribution ratios of each mode to the response changes with the iteration of the growth analysis. As a result, the change of natural frequencies was not

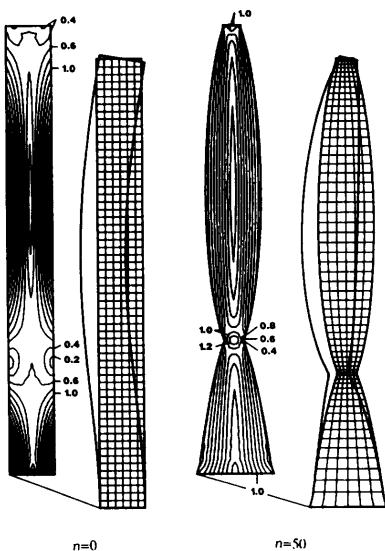


(a) meshes, mode shapes and contours of Mises stress normalized with volume average

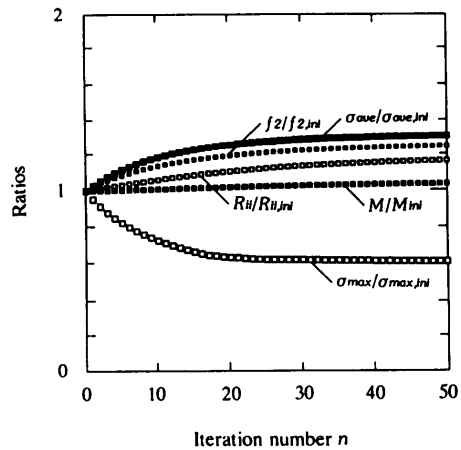


(b) convergence rates to initial values: maximum Mises stress  $\sigma_{max}$  evaluated at Gaussian points, volume average of Mises stress  $\sigma_{ave}$ , mass  $M$ , natural frequency  $f_1$  of 1st mode ( $f_{1, ini}=61.6$  Hz) and self-residue  $R_{ii}$  at center point  $i$  on top surface

Fig. 3 Results with 1st mode in Case 1.



(a) meshes, mode shapes and contours of Mises stress normalized with volume average



(b) convergence rates to initial values: maximum Mises stress  $\sigma_{max}$  evaluated at Gaussian points, volume average of Mises stress  $\sigma_{ave}$ , mass  $M$ , natural frequency  $f_2$  of 2nd mode ( $f_{2, ini}=615.2$  Hz) and self-residue  $R_{ii}$  at center point  $i$  on top surface

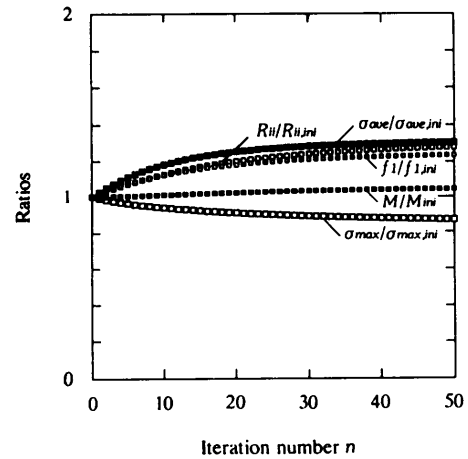
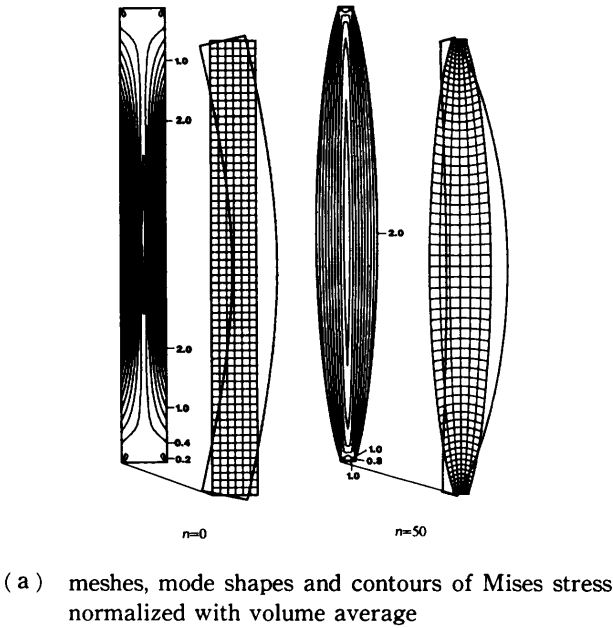
Fig. 4 Results with 2nd mode in Case 1

monotonous. However, the maximum value of the strength parameter, the mass and the deflection at the center of top surface monotonously converged. The maximum value of the strength parameter with which the strength is determined was reduced to 13% of the initial value.

4. Conclusions

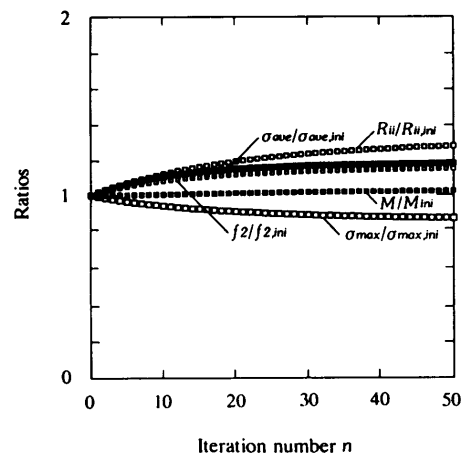
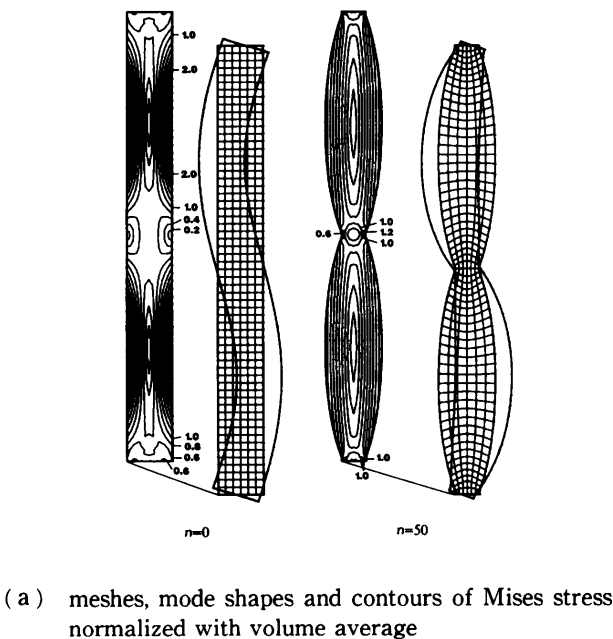
In the present report, a method for application of the growth strain method<sup>(1)</sup> to the problems of steady-state vibration was described. The growth

parameter with which the bulk strain is generated was assumed to be given with the strength parameter such as the Mises stress, and evaluated at the maximum deformation in steady-state vibration. From numerical examination on simple beam structures, we obtained the results that the maximum value of the strength parameter and the natural frequency monotonously converged in the free vibration with each normal mode, and that in the response to harmonic excitation, while the natural frequencies did not vary monotonously, the maximum value of the strength



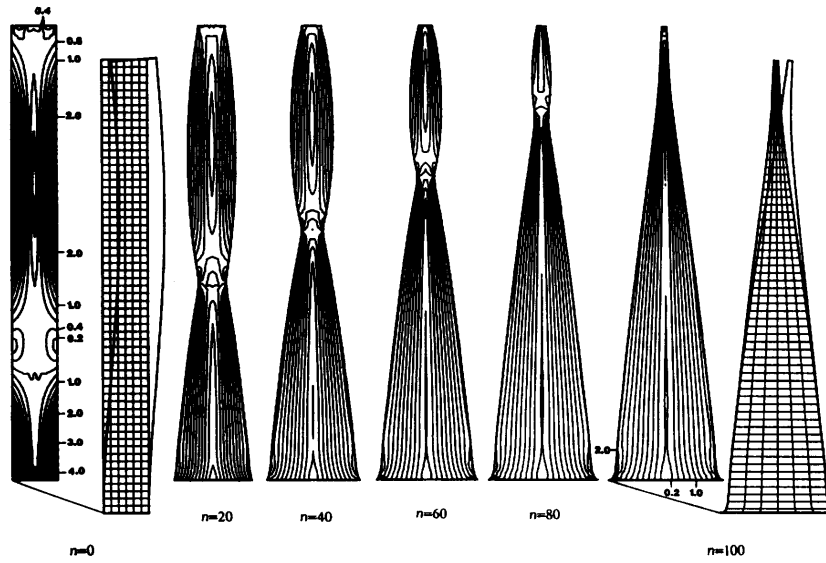
(b) convergence rates to initial values: maximum Mises stress  $\sigma_{max}$  evaluated at Gaussian points, volume average of Mises stress  $\sigma_{ave}$ , mass  $M$ , natural frequency  $f_1$  of 1st mode and self-residue  $R_{ii}$  at center point  $i$  of top surface

Fig. 5 Results with 1st mode in Case 2

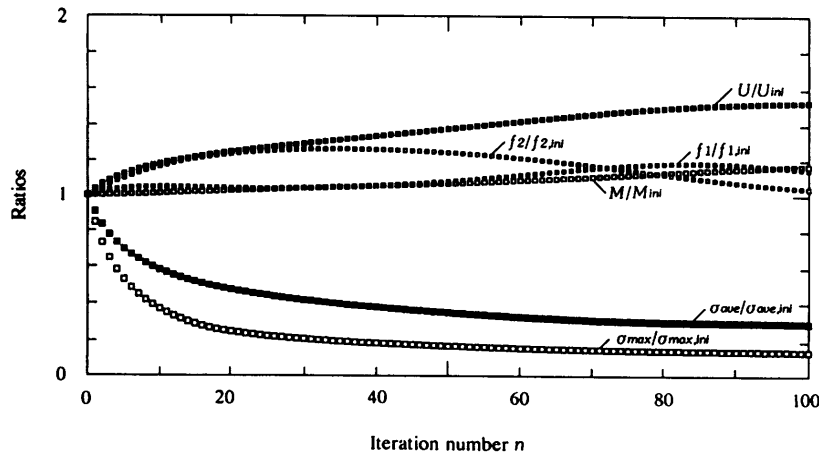


(b) convergence rates to initial values: maximum Mises stress  $\sigma_{max}$  evaluated at Gaussian points, volume average of Mises stress  $\sigma_{ave}$ , mass  $M$ , natural frequency  $f_2$  of 2nd mode and self-residue  $R_{ii}$  at center point  $i$  on top surface

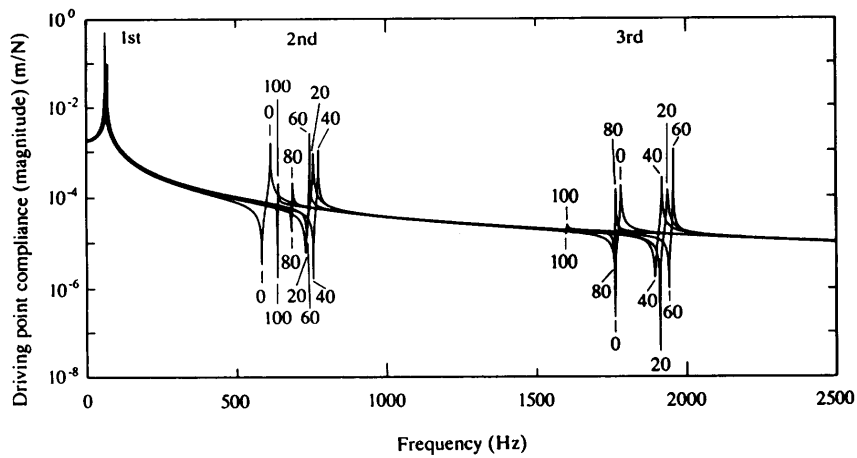
Fig. 6 Results with 2nd mode in Case 2



(a) meshes, response shapes and contours of Mises stress normalized with volume average



(b) convergence rates to initial value : maximum Mises stress  $\sigma_{max}$  evaluated at Gaussian points, volume average of Mises stress  $\sigma_{ave}$ , mass  $M$ , natural frequency  $f_r$  of  $r$ -th mode and amplitude of displacement  $U$  at center point on top surface



(c) self-transfer function at center point on top surface

Fig. 7 Results in Case 3

parameter with which the strength is determined steadily converged.

#### References

- (1) H. Azegami, A Proposal of a Shape-Optimization Method Using a Constitutive Equation of Growth (In the Case of a Static Elastic Body), *JSME Int. J., Series 1*, Vol. 33, No. 1 (1990), p. 64.
- (2) Niordson, F. I., On the Optimal Design of a Vibrating Beam, *Q. Appl. Math.*, Vol. 23, No. 1 (1965), p. 47.
- (3) Turner, M. J., Design of Minimum Mass Structures, with Specified Natural Frequencies, *AIAA J.*, Vol. 5, No. 3 (1967), p. 406.
- (4) Taylor, J. E., Minimum Mass Bar for Axial Vibration at Specified Natural Frequency, *AIAA J.*, Vol. 5, No. 10 (1967), p. 1911.
- (5) Brach, R. M., On the Extremal Fundamental Frequencies of Vibrating Beams, *Int. J. Solids Struct.* Vol. 4, No. 2 (1968), p. 667.
- (6) Fox, R. L., and Kapoor, M. P., Structural Optimization in the Dynamic Respose Regime: A Computational Approach, *AIAA J.*, Vol. 8, No. 10 (1970), p. 1798.
- (7) Olthoff, N., Optimal Design of Vibrating Rectangular Plates, *Int. J. Solids Struct.*, 10 (1974), p. 93.
- (8) Tada, Y., Seguchi, Y., Shape Determination of Structures Based on the Inverse Variational Principle/The Finite Element Approach, *New Directions in Optimum Structural Design*, Edited by E. Atrek, R. H. Gallager, K. M. Ragsdell and O. C. Zienkiewicz, John Wiley & Sons Ltd. (1984), p. 197.
- (9) Yamakawa, H., Optimum Structural Designs for Dynamic Response, *New Directions in Optimum Structural Design*, Edited by E. Atrek, R. H. Gallager, K. M. Ragsdell and O. C. Zienkiewicz, John Wiley & Sons Ltd. (1984), p. 249.